Available online at www.sciencedirect.com

ScienceDirect

Procedia Manufacturing 47 (2020) 1456–1461

Procedia MANUFACTURING

www.elsevier.com/locate/procedia

23rd International Conference on Material Forming (ESAFORM 2020)

Modelling Anisotropic Behavior of AISI 304 Stainless Steel Sheet Using a Fourth-Order Polynomial Yield Function

Bora Sener[a], Elif Sila Kilicarslan[b], Mehmet Firat[c,*]

[a]*Yildiz Technical University, Istanbul, 34349, Turkey*
[b]*Istanbul Gedik University, Istanbul, 34876, Turkey*
[c]*The University of Sakarya, Sakarya,54020, Turkey*

* Corresponding author. Tel.: +90(264) 295 58 80; fax: +90(264) 295 58 50. *E-mail address:* firat@sakarya.edu.tr

Abstract

Following the description of an orthotropic, non-quadratic, homogenous polynomial type yield criterion, its finite element (FE) implementation is presented for the purpose of sheet metal forming analysis using an explicit time integration scheme. Then the performance of the FE implementation is firstly investigated by means of tensile test simulations of AISI (304) stainless steel sheets, and directional variation of yield strength and anisotropy factors are predicted. Next, deep drawing simulations of rectangular cups are performed, and FE computed cup thickness and flange geometry are assessed with measurements. Comparisons in both deformation processes showed that a fourth-order polynomial criterion can accurately describe the anisotropic behavior of AISI (304) stainless steel sheets.

Keywords: Polynomial type yield function; Finite element simulation; Rectangular cup drawing; AISI-304 steel sheet

1. Introduction

Accurate description of material anisotropy is required to obtain reliable results from the finite element (FE) simulations of sheet metal forming processes. Plastic behavior of sheet metal is defined by plane stress orthotropic yield criteria. The first anisotropic yield criterion was proposed by Hill [1]. Hill48 yield function has a simple formulation and its coefficients are determined with explicit formulas. Therefore, the quadratic criterion is considered as a universal criterion in the literature. However, Hill48 criterion can't accurately predict both the directional variation of the yield stress and plastic strain ratios of the material. Due to the limitations of his quadratic criterion, he later suggested the use of general homogeneous polynomials as yield functions [2].

Polynomial type yield functions were firstly investigated by Gotoh [3]. He proposed the fourth order polynomial as the yield function and derived a nine by nine system of linear equations to determine the polynomial coefficients in his study. Then he used the criterion in modelling of anisotropic behavior of commercial Al-killed steel and Cu-(1/4)H sheets and successfully predicted variations in directional properties of these materials [4]. However, author didn't consider the positivity and convexity of the yield function in the coefficient identification procedure. Therefore, Gotoh's yield criterion has not been widely used in sheet metal forming analyses [5]. Tong [6] reformulated Gotoh's yield function as a part of the fourth order Hill1979 [7] yield function and verified the positivity and convexity conditions of the function. Cazacu and Barlat [8] proposed the six-order polynomial yield function (CB2001) based on the extension of Drucker's isotropic yield criterion and predicted the planar variations of mechanical properties of face centered cubic (FCC) materials. However, the coefficient identification procedure of CB2001 yield criterion depend on complicated nonlinear formulas. Hu [9-10] proposed two polynomial yield functions for 2D and 3D cases respectively.

10.1016/j.promfg.2020.04.320

He applied the criteria in modelling of high strength steels and aluminum alloys and predicted the planar distributions of the yield stress and plastic strain ratios of the materials. Researchers have met with difficulties when implementing the polynomial yield functions into a FE code due to the convexity issues. In order to remove this constraint, Soare [11] has proposed a different coefficient identification procedure for the polynomial type yield functions and successfully applied the criteria in the earing prediction.

In this study, the prediction capability of the fourth-order polynomial yield criterion (Poly4) developed by Soare was evaluated. Firstly, the planar variations of the yield stress and plastic strain ratios of the material were predicted, then FE simulation of a rectangular cup drawing process was performed to evaluate the criterion. Finally, the computed results were compared with experimental results. AISI-304 steel sheet (t = 0.8mm) was chosen as a test material.

The article consists of six sections: Section 2 briefly introduces the fourth-order polynomial yield criterion. Section 3 and Section 4 give information about the experimental studies and FE model of the rectangular cup drawing process, respectively. Section 5 compares the numerical results with experiment. Finally, Section 6 presents a summary and discussion of the results obtained from this study.

Nomenclature

t	Thickness of the blank
a_1-a_9	The coefficients of the fourth order polynomial yield criterion
$\bar{\sigma}_0, \bar{\sigma}_{45}$ *and* $\bar{\sigma}_{90}$	Yield stress ratios in three different directions
$\bar{\sigma}_b$	Biaxial yield stress ratio
$\bar{\sigma}_\theta$	Yield stress ratio in θ direction
r_0, r_{45}, r_{90}	Plastic strain ratios in three different directions
ψ	Error function
w_1, w_2	Weight coefficients in the error function
K	Strength coefficient
n	Strain hardening exponent
ε_0	Initial plastic strain

2. The fourth order polynomial yield function

2.1. A fourth order homogenous polynomial type yield criterion

The fourth order polynomial yield criterion was developed by Soare. The criterion has 9 coefficients for the plane stress case and can be written in the following form:

$$P_4 = a_1\sigma_x^{\ 4} + a_2\sigma_x^{\ 3}\sigma_y + a_3\sigma_x^{\ 2}\sigma_y^{\ 2} + a_4\sigma_x\sigma_y^{\ 3} + a_5\sigma_y^{\ 4} + \left(a_6\sigma_x^{\ 2} + a_7\sigma_x\sigma_y + a_8\sigma_y^{\ 2}\right)\sigma_{xy}^{\ 2} + a_9\sigma_{xy}^{\ 4} \quad (1)$$

Soare proposed modifications to Gotoh's identification program and developed a coefficient identification procedure based on the positivity and convexity of the yield surface. According to Soare's coefficient identification program, the five coefficients (a_1, a_2, a_3, a_4 and a_5) can be determined with explicit formulas, the coefficients a_6 and a_8 can be found by minimizing the error function and finally the coefficient a_7 is computed based on the coefficients a_6 and a_8. Also, he derived upper and lower bounds on coefficients to obtain a positive and convex yield function.

Eleven experimental inputs ($\bar{\sigma}_0, \bar{\sigma}_{45}, \bar{\sigma}_{90}, \bar{\sigma}_b, r_0, r_{45}, r_{90}$ and $\bar{\sigma}_\theta$ and r_θ for $\theta = 15^0$ and 75^0 (or 30^0 and 60^0)) are required to determine the $a_{1\text{-}9}$ coefficients. Required mathematical expressions for determination of these coefficients are given as follows:

$$a_1 = 1, a_2 = -4r_0/\left(1+r_0\right), a_5 = 1/\bar{\sigma}_{90}^4 \quad (2)$$

$$a_4 = -4a_5\, r_{90}/\left(1+r_{90}\right), a_3 = \left(1/\bar{\sigma}_b^4\right) - \left(a_1 + a_2 + a_4 + a_5\right) \quad (3)$$

$$a_6 = (k_{22}r_1 - k_{12}r_2)/(k_{11}k_{22} - k_{12}^2), a_8 = (k_{22}r_2 - k_{12}r_1)/(k_{11}k_{22} - k_{12}^2) \quad (4)$$

$$a_7 = [\left(2/\bar{\sigma}_{45}^4\right)/(1+r_{45}) - 2\left(1/\bar{\sigma}_b^4\right)] - \left(a_6 + a_8\right) \quad (5)$$

Where k_{11}, k_{22}, k_{12}, r_1 and r_2 parameters are determined by the minimization of the error function which evaluates the difference between the estimated values and the experimental ones. These parameters are given below:

$$k_{11} = \sum_{i=1,2}\left[w_1^{(i)}\left(\alpha_6^i\right)^2 + w_2^{(i)}\left(\beta_6^i\right)^2\right], k_{22} = \sum_{i=1,2}\left[w_1^{(i)}\left(\alpha_8^i\right)^2 + w_2^{(i)}\left(\beta_8^i\right)^2\right] \quad (6)$$

$$k_{12} = \sum_{i=1,2}\left(w_1^{(i)}\alpha_6^i\alpha_8^i + w_2^{(i)}\beta_6^i\beta_8^i\right) \quad (7)$$

$$r_1 = \sum_{i=1,2}\left(w_1^{(i)}\alpha_6^i\alpha_0^i + w_2^{(i)}\beta_6^i\beta_0^i\right), r_2 = \sum_{i=1,2}\left(w_1^{(i)}\alpha_8^i\alpha_0^i + w_2^{(i)}\beta_8^i\beta_0^i\right) \quad (8)$$

Where $w_1^{(i)}$ weights the data points $\bar{\sigma}_\theta$,whereas $w_2^{(i)}$ weights the data points r_θ at the locations θ_i . $\alpha^{(i)}$ and $\beta^{(i)}$ in the above formulas are the coefficients appearing in the expression of the error function. $\bar{\sigma}_\theta$ and r_θ indicate that yield stress and plastic strain ratios at the angle θ with respect to the rolling direction, respectively. σ_0 is accepted as reference yield stress in the determination of stress ratios $\left(\bar{\sigma}_\theta = \sigma_\theta/\sigma_0\right)$. Detailed information for the coefficient identification program of the criterion is given in [11].

In this study, a different identification procedure from Soare was used and trust region approach was applied in the minimization of error function. Trust region algorithm reduces the objective value significantly and can handle the case of singularity of Jacobian [12]. The flow chart of the fourth-order polynomial yield criterion is shown in Fig. 1.

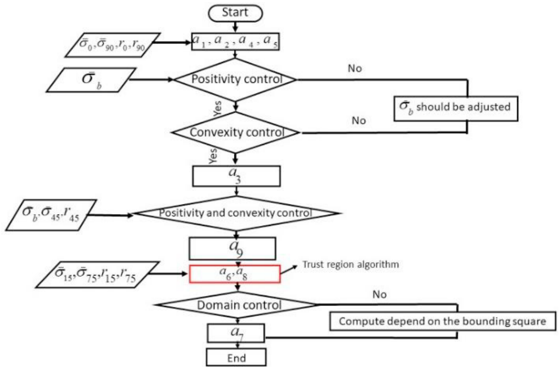

Fig. 1. Flow chart of the fourth order polynomial yield criterion.

2.2. Finite element (FE) implementation

The fourth order homogenous polynomial type yield criterion is implemented into the commercial dynamic explicit FE software Ls-Dyna971 through the user defined material subroutine Umat43 [13]. The process simulation models of sheet metal forming applications necessitates a large strain and finite rotation formulation of FE discrete equations and Ls-Dyna program uses an Updated Lagrangian formulation based on the use of corotational rotation-neutralized stress and strain measures [13,14]. Accordingly, the reference state for the computation of increments of stress and strain is the end of the time step for which the equilibrium is sought, and the large deformation kinematics is decoupled from constitutive response in the case of finite strain elastic-plastic material deformation.

The program provides, to Umat subroutine, the rotation-neutralized strain increment as output and inputs the convergent stress increment computed via the constitutive model that uses the given strain increment as the basic input. Finite element analyses necessitate the time integration of the plasticity equations at each integration point in the finite element model and termed as "local integration" problem [14, 15]. In order to compute the stress increment for a given rotation-neutralized strain increment the ordinary differential equations describing the incremental stress-strain relations are discretized in time using Backward Euler method [16,17]. Next, a nonlinear scalar function is used to describe a convergence condition for increment of accumulated plastic strain for a given time step. The nonlinear scalar equation is solved iteratively by a successive substitution and updating the total backstress and yield function during iterations. Once the convergence to increment of accumulated plastic strain for a given time step is found, the stress and strain tensors at the end of time step are updated and returned to Umat subroutine.

3. Experimental studies

3.1. Uniaxial tensile test

Yield stresses and plastic strain ratios of the material were obtained from the uniaxial tensile tests performed in three different directions (rolling, diagonal and transverse). Tests were carried out at an equivalent strain rate of $0.008s^{-1}$ and were repeated three times to provide reproducibility.

The experimental yield stress and plastic strain ratios in three directions are given in Table 1. Yield stress of the material along the rolling direction is 309.86 MPa.

Table 1. Experimental data for AISI-304 steel.

Directional properties	0^0	45^0	90^0	Biaxial
Yield stress ratio	1.000	0.947	0.979	0.9611
Plastic strain ratio (r)	0.822	1.104	0.798	-

Biaxial yield stress of the material was taken from the literature [18]. 15^0 and 75^0 were accepted as interval angles in the coefficient identification procedure of the fourth order polynomial yield criterion and these angles were determined by using the following equations:

$$\sigma_{30} = (\sigma_0 + \sigma_{45})/2, \sigma_{15} = (\sigma_0 + \sigma_{30})/2 \tag{9}$$

$$\sigma_{60} = (\sigma_{30} + \sigma_{90})/2, \sigma_{75} = (\sigma_{60} + \sigma_{90})/2 \tag{10}$$

3.2. Drawing of a rectangular cup

Rectangular cup drawing process was considered as case study for evaluating the modeling capability of the fourth order polynomial yield criterion. Experiments were carried out on a 160t capacity double action hydraulic press. Mineral oil was used as lubricant and it was applied on the blank-die and blank-binder interfaces. Rectangular cup which has 80 mm height was successfully formed with 340kN binder force (BF) and 20 mm/s die velocity. Experimental set-up and the formed part were shown in Fig. 2. After the test, the formed parts were cut through rolling, diagonal and transversal directions. Then, thickness distributions for each direction were measured by micrometer. In addition, the formed parts were scanned to capture the flange profiles of the cups.

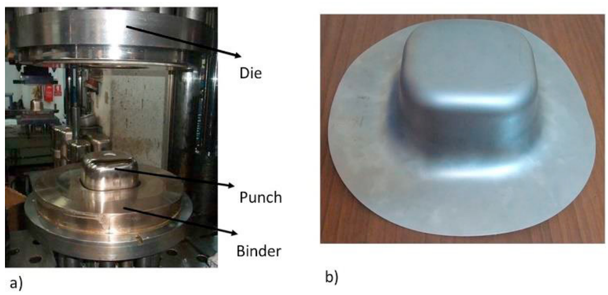

Fig. 2. (a) Experimental set-up; (b) the formed part.

4. FE model

Rectangular cup deep drawing process was modeled by using nonlinear explicit FE code Ls-Dyna. Only a quarter of the parts were modelled due to the symmetry conditions.

Strain hardening behavior of the material was defined with Swift isotropic hardening law. Hardening parameters were determined by fitting to the results of tensile tests in rolling direction and are given in Table 2.

Table 2. Hardening parameters of AISI-304 steel.

Material	K *(MPa)*	ε_0	n
AISI 304	1349	0.00178	0.316

Forming-one-way-surface-to-surface contact algorithm was used for defining of contact between the blank and the tools. Friction coefficient was taken as 0.05 at the blank-die and blank-binder interfaces due to application of mineral oil, while it was taken as 0.125 at the blank-punch interface due to dry condition. The die motion was defined as displacement controlled and 85kN BF was applied in FE simulations due to the quarter model. The BF-time and die displacement-time curves defined in the FE model were shown in Fig. 3. It was shown from the Fig. 3 that BF reached 85kN at time = 0.1s and the motion of the die was delayed by 0.115s to stabilize the BF and reduce the oscillations in the blank.

The blank was modeled using full integrated quadrilateral shell elements with five integration points. The general mesh pattern is shown in Fig. 4.

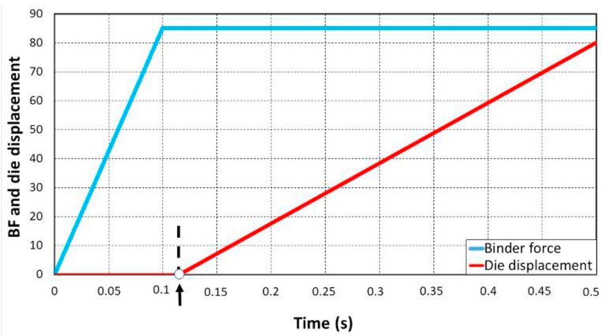

Fig. 3. Binder force and die displacement curves.

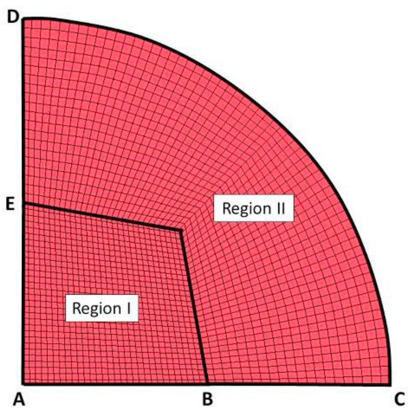

Fig. 4. General mesh pattern of the blank.

Mesh sensitivity study was performed to find the optimum mesh size. The blank was divided into two regions and four different mesh densities were considered for this study. Von Mises yield criterion (*MAT18) was used in mesh sensitivity study. Values for regions shown in Fig. 4 corresponding to each of case studies are summarized in Table 3.

Table 3. Mesh densities used in mesh refinement study.

Case No	Number of elements per line segments		
	AB and AE	BC and ED	CD
Case 1	10	10	20
Case 2	20	10	40
Case 3	30	20	60
Case 4	40	20	80

FE simulations were performed for each case. The penetrations between the blank and the punch were observed on the first two simulations due to coarse mesh of the blank (Fig. 5). Therefore, the mesh sizes in both Case1 and Case 2 were not considered in the study.

In order to evaluate Case3 and Case4, minimum and maximum thickness values were considered and the results for two different meshes are presented in Table 4. As it is seen from Table 4 that the simulation results of Case3 and Case4 were similar and reducing the mesh size will not significantly affect the solution. Therefore, the mesh size in Case 3 (3 mm) was considered as optimum size in the study. After determining the optimum mesh size, FE analyses were carried out with the fourth order polynomial yield criterion. The criterion was implemented in explicit FE code Ls-Dyna by means of a user defined material subroutine (UMAT).

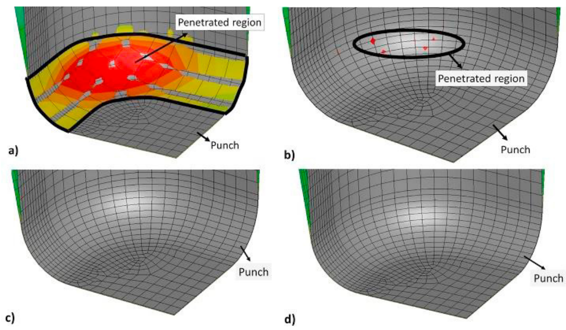

Fig. 5. FE simulation results (a) Case 1; (b) Case 2; (c) Case 3; (d) Case 4.

Table 4. Minimum and maximum thickness values for Case3 and Case4.

Case number	Min. thickness (*mm*)	Max. thickness (*mm*)
Case 3	0.522	0.867
Case 4	0.520	0.866

5. Results

In this section, the predicted results from the yield criterion are compared with experimental results to evaluate the prediction capability of the criterion. Comparisons were carried out in two stages: In the first stage, angular variations of yield stress and plastic strain ratios were considered. In the second stage, FE results namely, a) thickness distributions and b) the flange geometry were compared with experiments.

5.1. Angular variations of directional properties

Angular variations of yield stress and plastic strain ratios were predicted with the fourth order polynomial yield criterion. The variations of these mechanical properties with respect to the angle in the sheet plane are calculated by using Eq. (11) and Eq. (12), respectively.

$$\bar{\sigma}_\theta = \sigma_\theta/\sigma_0 = 1/f\left(\cos^2\theta, \sin^2\theta, \sin\theta\cos\theta\right) \tag{11}$$

$$r_\theta = [(\partial f/\partial\sigma_{12})\sin\theta\cos\theta - (\partial f/\partial\sigma_{11})\sin^2\theta - (\partial f/\partial\sigma_{22})\cos^2\theta] / (\partial f/\partial\sigma_{11} + \partial f/\partial\sigma_{22}) \tag{12}$$

The parameters of the yield criterion were determined by using experimental data given in Table 1. As stated in Section 2, trust region algorithm was used in the minimization of error function which is used to determine a_6 and a_8 coefficients of the fourth order polynomial yield criterion. Minimization trials were conducted with various weight coefficients and the optimum weights were found as follows:

$$w_1^{(1)} = w_1^{(2)} = 7, w_2^{(1)} = 0.04, w_2^{(2)} = 0.09\,. \tag{13}$$

Determined parameters of the fourth order polynomial yield criterion are presented in Table 5.

Table 5. The coefficients of the fourth order polynomial yield criterion.

a_1	a_2	a_3	a_4	a_5	a_6	a_7	a_8	a_9
1.000	-1.805	2.818	-1.928	1.086	5.958	-5.650	6.811	11.619

After determining of the coefficients, angular variations of the directional properties were predicted. Comparisons between experimental and theoretical variations of the yield stress and plastic strain ratios are shown in Fig. 6 and Fig. 7, respectively.

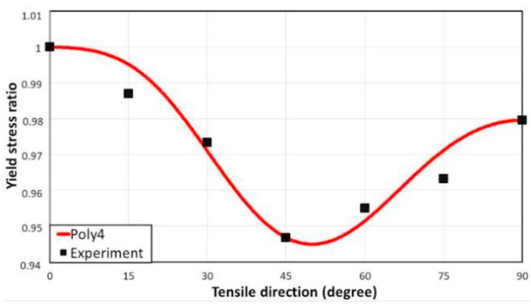

Fig. 6. Comparison of predicted and experimental yield stress ratios.

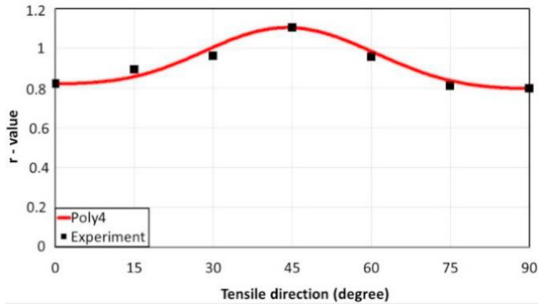

Fig. 7. Comparison of predicted and experimental plastic strain ratios.

After comparison of the predicted and experimental yield stress and plastic strain ratios, the contours of the yield loci were plotted in different shear stresses as shown in Fig. 8.

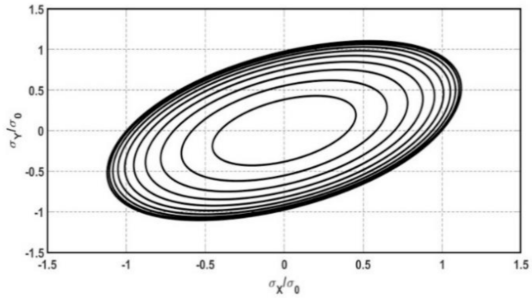

Fig. 8. The contours of the Poly4 yield loci in different shear stresses

As it is shown from the Fig. 8 that the contours of yield loci are convex and also they have oval shape near equibiaxial stress state.

5.2. FE results

FE analyses of the rectangular cup drawing process were performed by using the fourth order polynomial yield criterion. Predicted thickness distributions along three directions (rolling, diagonal and transverse) and flange geometry were compared with experiments. Results are given in Figure 9-12.

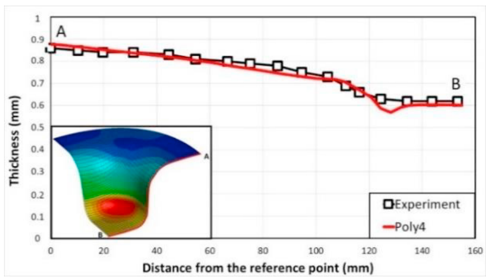

Fig. 9. Comparison of predicted and experimental thickness distributions in rolling direction.

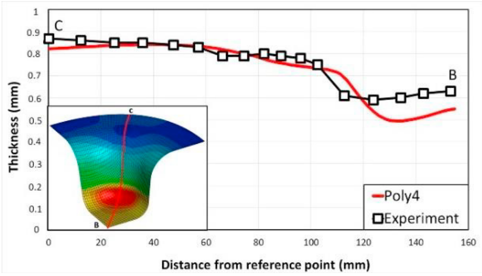

Fig. 10. Comparison of predicted and experimental thickness distributions in diagonal direction.

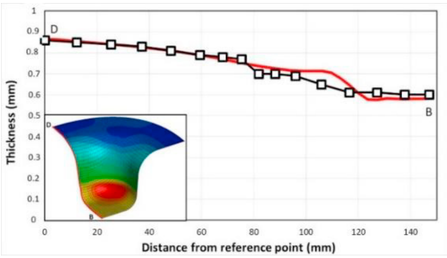

Fig. 11. Comparison of predicted and experimental thickness distributions in transverse direction.

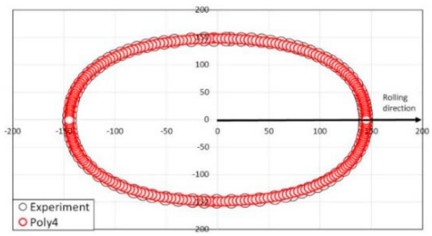

Fig. 12. Comparison of predicted and experimental flange geometries.

It is seen from the figures that the predicted thickness distributions in three directions and the flange geometry agree well with the experimental results.

6. Summary

Modeling capability of the fourth-order polynomial yield criterion was evaluated in this study. The criterion was implemented into explicit FE code Ls-Dyna by using user defined material model (UMAT) and applied to the rectangular cup drawing simulation of AISI 304 steel sheet. Firstly, the planar variations of the yield stress and plastic strain ratios and then thickness distributions in three different directions and flange geometry were predicted. From the comparison of theoretical and experimental results, the following conclusions could be drawn:

- From the angular variations of directional properties, it was understood that the fourth order polynomial yield function could successfully describes the variations of the yield stress and plastic strain ratios in the plane of the blank.
- From the contours of yield loci, it was observed that Poly4 yield locus are convex and this indicated that determined coefficients satisfy the convexity conditions.
- From the FE simulation results, it is seen that the thickness distributions in three directions and the flange geometry can be predicted with very high precision by using Poly4 yield criterion.
- From these comparisons, it is shown that Poly4 yield criterion can be successfully used for modeling of anisotropic behavior of AISI-304 steel sheets.

Acknowledgements

The authors would like to thank Oztiryakiler Company for the using of their equipment.

References

[1] Hill R. A theory of the yielding and plastic flow of anisotropic metals. Proc Soc London A 1948;193A:281-97.
[2] Hill R. The mathematical theory of plasticity. 1st ed. New York: Oxford University Press Inc; 1950.
[3] Gotoh M. A theory of plastic anisotropy based on a yield function of fourth order (plane stress state)-I. Int J Mech Sci 1977;19:505-12.
[4] Gotoh M. A theory of plastic anisotropy based on yield function of fourth order (plane stress state)-II. Int J Mech Sci 1977;19:513-20.
[5] Tong W. On the certification of positive and convex Gotoh's fourth-order yield function. Numisheet Conf Series 2018;1063:1-6.
[6] Tong W. Generalized fourth-order Hill's 1979 yield function for modeling sheet metals in plane stress. Acta Mech 2016;227:2719-33.
[7] Hill R. Theoretical plasticity of textured aggregates. Math Proc Camb Philos Soc 1979;85:179-91.
[8] Cazacu O, Barlat F. Generalization of Drucker's yield criterion in orthotropy. Math Mech Solids 2001;6:613-630.
[9] Hu W. Characterized behaviors and corresponding yield criterion of anisotropic sheet metals. Mat Sci Eng A 2003;345:139-44.
[10] Hu W. An orthotropic yield criterion in a 3-D general stress state. Int J Plast 2005;21:1771-96.
[11] Soare SC, Yoon JW, Cazacu O. On the use of homogeneous polynomials to develop anisotropic yield functions with applications to sheet forming. Int J Plast 2008;24:915-44.
[12] Suan W, Yuan YX. Optimization theory and methods nonlinear programming. Springer Science Business Media; 2006.
[13] Hallquist JO. Ls-Dyna Theory Manual. Livermore Software Technology Corporation; 2006.
[14] Simo JC, Hughes TJR. Computational Inelasticity. New York: Springer-Verlag New York Inc; 1998.
[15] Chaboche JL, Cailletaud G. Integration methods for complex plastic constitutive equations. Comput. Method Appl Mech Eng 1996;133:125-55.
[16] Firat M, Kaftanoglu B, Eser O. Sheet metal forming analyses with an emphasis on the springback deformation. J Mater Process Tech 2008;196:135-48.
[17] Firat M. Computer aided analysis and design of sheet metal forming processes: Part III: Stamping die-face design. Mater Design 2007;28(4):1311-20.
[18] Yadav AD. Process analysis and design in stamping and sheet hydroforming. Doctoral Thesis 2008.